Title

Cationic Effects on the Net Hydrogen Atom Bond Dissociation Free Energy of High-Valent Manganese Imido Complexes

Journal

Journal of the American Chemical Society, 144(4)

ISSN

0002-7863

Authors

Léonard, Nadia G
Chantarojsiri, Teera
Ziller, Joseph W
et al.

Publication Date

2022-02-02

DOI

10.1021/jacs.1c09583

Peer reviewed

HHS Public Access

Author manuscript

J Am Chem Soc. Author manuscript; available in PMC 2022 May 19.

Published in final edited form as:

J Am Chem Soc. 2022 February 02; 144(4): 1503–1508. doi:10.1021/jacs.1c09583.

Cationic Effects on the Net Hydrogen Atom Bond Dissociation Free Energy of High-Valent Manganese Imido Complexes

Nadia G. Léonard,
Department of Chemistry, University of California, Irvine, California 92697, United States

Teera Chantarojsiri,
Department of Chemistry and Center of Excellence for Innovation in Chemistry, Faculty of Science, Mahidol University, Bangkok 10400, Thailand

Joseph W. Ziller,
Department of Chemistry, University of California, Irvine, California 92697, United States

Jenny Y. Yang
Department of Chemistry, University of California, Irvine, California 92697, United States; Pacific Northwest National Laboratory, Richland, Washington 99352, United States

Abstract

Local electric fields can alter energy landscapes to impart enhanced reactivity in enzymes and at surfaces. Similar fields can be generated in molecular systems using charged functionalities. Manganese(V) salen nitrido complexes (salen = *N*,*N*′-ethylenebis(salicylideneaminato)) appended with a crown ether unit containing Na^+ (**1-Na**), K^+, (**1-K**), Ba^{2+} (**1-Ba**), Sr^{2+} (**1-Sr**), La^{3+} (**1-La**), or Eu^{3+} (**1-Eu**) cation were investigated to determine the effect of charge on pK_a, $E_{1/2}$, and the net bond dissociation free energy (BDFE) of N–H bonds. The series, which includes the manganese(V) salen nitrido without an appended crown, spans 4 units of charge. Bounds for the pK_a values of the transient imido complexes were used with the Mn(VI/V) reduction potentials to calculate the N–H BDFEs of the imidos in acetonitrile. Despite a span of >700 mV and >9 pK_a units across the series, the hydrogen atom BDFE only spans ~6 kcal/mol (between 73 and 79 kcal/mol). These results suggest that the incorporation of cationic functionalities is an effective strategy for accessing wide ranges of reduction potentials and pK_a values while minimally affecting the BDFE, which is essential to modulating electron, proton, or hydrogen atom transfer pathways.

Corresponding Author Jenny Y. Yang – Department of Chemistry, University of California, Irvine, California 92697, United States; Pacific Northwest National Laboratory, Richland, Washington 99352, United States; j.yang@uci.edu.

Author Contributions

The manuscript was written through contributions of all authors. All authors have given approval to the final version of the manuscript.

Supporting Information

The Supporting Information is available free of charge at https://pubs.acs.org/doi/10.1021/jacs.1c09583.

Experimental procedures and spectroscopic data (PDF)

Accession Codes

CCDC 2108907–2108908 contain the supplementary crystallographic data for this paper. These data can be obtained free of charge via www.ccdc.cam.ac.uk/data_request/cif, or by emailing data_request@ccdc.cam.ac.uk, or by contacting The Cambridge Crystallographic Data Centre, 12 Union Road, Cambridge CB2 1EZ, UK; fax: +44 1223 336033.

The authors declare no competing financial interest.

The activation of strong heteroatom–hydrogen (X–H) bonds using high-valent metal oxidos or nitridos as hydrogen atom acceptors is a robust area of bioinspired reaction chemistry.[1-4] The free energy of these reactions is dependent on the hydrogen atom bond dissociation free energies (BDFEs) for the reactants and products. BDFE values are comprised of both the pK_a and redox potential ($E_{1/2}$) according to eq 1 (Chart 1).[5-7] Exergonic reactivity with metal oxidos/nitridos requires the BDFE values for the resultant hydroxido/imido bonds to exceed that of the targeted X–H bond. However, the *relative contributions* of pK_a and $E_{1/2}$ to the BDFE are also critical for steering reactivity.[8,9] The difference in reduction potential ($\Delta E_{1/2}$) and pK_a (ΔpK_a) between the donor and acceptor governs the most favorable reaction pathway for proton, electron, or concerted hydrogen atom transfer (HAT).[10-12] In some cases, the rate of HAT correlates more strongly with $\Delta E_{1/2}$ or ΔpK_a than with $\Delta G(H^{\bullet})$,[13-15] deviating from the Bell–Evans–Polanyi principle that the overall free energy governs kinetic reactivity.[16,17] This occurrence can lead to a kinetic selectivity for the cleavage of stronger X–H bonds in the presence of weaker bonds. Thus, understanding how synthetic variations modify the reduction potential, pK_a, and consequential BDFE is critical for controlling HAT reactions.[18]

Most studies have used inductive effects to modulate these quantities, leading to modest changes; an alternative approach is to use the secondary coordination sphere. Borovik and co-workers used hydrogen-bond donation from an amide ligand to demonstrate basicity-controlled HAT to a manganese oxido (Figure 1a, left).[19] Tolman and co-workers found that the incorporation of sulfonate or trimethylammonium substituents expands the range of the Cu(III/II) reduction potential ($E_{1/2}$) by 275 mV in Cu(II) hydroxide complexes (Figure 1a, right).[20] Despite the change in $E_{1/2}$, the BDFE of the Cu(II) aqua species remained relatively constant while the kinetics of hydrogen atom transfer to the Cu(III) hydroxide varied, which is attributed to steric contributions of the counterions in addition to possible electrostatic effects. Thus far, direct correlations between changes in thermochemical parameters and electrostatic effects at molecular complexes have been minimally explored.[21-24]

In this study, we report the effect of proximal mono-, di-, and trications on high-valent Mn nitrido complexes and the hydrogen atom BDFEs of their associated imidos. Manganese nitrido complexes are used in many catalytic and stoichio-metric reactions that form intermediate imidos (Figure 1b).[27-46] Although their BDFEs are central in catalytic nitrogen cycles[47-52] and C–H activation,[53-58] few values have been measured in comparison to isoelectronic metal oxido analogues. The salen-crown framework provides a unique platform for isolating the effect of the cationic charge on the metal center (Chart 1). Non-redox-active cations in the crown modify the electric field potential around the redox-active metal.[25] Our previous investigation with complexes **1-Na**, **1-K**, **1-Ba**, and **1-Sr** exhibited anodic shifts of over 400 mV of the Mn(VI/V) reduction potential (Table 1) with increasing cationic charge.[26]

We have now synthesized two derivatives with +3 cations, **1-La** and **1-Eu**, so that our series spans four different units of charge (see the Supporting Information). Single crystals suitable for X-ray diffraction of **1-La** (Figure 2a) and **1-Eu** (Figure S32) were obtained from concentrated acetonitrile solutions.

The electrochemical properties of **1-La** and **1-Eu** were measured in acetonitrile using cyclic voltammetry (Figure 2b and the Supporting Information). We previously described the bimolecular coupling of the oxidized Mn(VI) species to form 2 equiv of the corresponding Mn(III) complex and N_2 or an EC mechanism (electron transfer, chemical step) (Figure 1b-ii).[26,30] Lau and Man recently reported the reactivity of a Mn(VI) nitrido complex that was also isolated and structurally characterized despite undergoing similar bimolecular reactivity.[59] In our prior study with the mono- and dicationic nitrido complexes, an increase in charge corresponded to a slower rate of bimolecular coupling. Consistent with this trend, there is no evidence of bimolecular coupling upon oxidation of **1-La** to Mn(VI) even at slow scan rates (10 mV/s) (Figure 1b and Figures S16 and S17). The redox event is reversible, and there is no reduction event corresponding to the Mn(III/II) couple at more negative potentials, which would be the expected product of bimolecular coupling.

On the basis of the oxidation event observed for **1-Eu**, the $E_{1/2}$ is about ~1.13 V. However, we note that the cathodic wave for the Mn(VI/V) redox couple is smaller than the anodic wave (Figure S19). There is evidence that, upon oxidation, adventitious Na^+ ions displace the europium(III) ions due to the latter's poor fit in the crown (ionic radii of 102 and 94.7 pm, respectively).[60] Analytically pure **1-Eu** was used for cyclic voltammetry and the **1-Na** oxidation peak was not observed in the initial oxidative scan. However, after several oxidation cycles, an additional cathodic redox feature appeared at ~0.6 V (vs $[Fe(C_5H_5)_2]^{+/0}$) (Figure S21), which matches the oxidation potential of the Mn(V) nitrido with Na^+ in the crown cavity.

The $E_{1/2}$ values for the Mn(VI/V) reduction potential of 1.02 V (**1-La**) and ~1.13 V (**1-Eu**) vs $[Fe(C_5H_5)_2]^{+/0}$ correspond to anodic shifts of 600 and 730 mV in comparison to the noncrown (salen)MnN (**A**) or changes of 14 and 16 kcal/mol, respectively, in the $E_{1/2}$ contributions to the N–H BDFE (eq 1 in Chart 1 and Figure 3).

We investigated the protonation of the manganese(V) nitrido complexes to determine the pK_a values. The direct detection and isolation of the parent electrophilic transition-metal imido complexes is challenging because of accessible coupling, disproportionation, and nitrene transfer pathways.[61-65] Acid titration experiments were conducted at room temperature or −35 °C in acetonitrile and were monitored by UV–vis spectroscopy through changes in two absorption bands associated with the manganese nitrido at ~380 and ~600 nm. No spectral features corresponding to a putative imido were observed.

Lau and co-workers previously discussed the instability of the imido formed following protonation of the nitride, where 2 equiv of the resulting imido complex couples to form a manganese(III) μ-diazene species, which rapidly decomposes to give the final Mn(III), N_2, and NH_3 (Figure 1b-i).[42] Indeed, in our studies the UV–vis spectrum at the end point of the acid titration corresponded to that of the Mn(III) complexes.

In an effort to observe the imido, we synthesized the ^{15}N-labeled nitrido complex **1-Ba(^{15}N)**. Protonation of **1-Ba(^{15}N)** with 1 equiv of $[H(OEt_2)_2][BF_4]$ in acetonitrile-d_3 was monitored by ^1H and ^{15}N NMR spectroscopy at −30 °C. Only resonances corresponding to the starting material and Mn(III) product were observed. An analysis of the gas headspace

following protonation of **1-Ba(15N)** showed $^{14}N^{15}N$ and $^{15}N_2$, further supporting the coupling pathway proposed by Lau. It is possible that, instead of protonating on the nitrido, nucleophilic attack at the imine of the salen could occur.[66-68] Alternatively, protonation of the crown ether could displace the bound cation.[69-71] However, these possibilities are unlikely, as there is quantitative recovery of the of the manganese(III) complex following protonation, indicating that the reactivity proceeds as shown in Figure 1.b-i.

The instability of the manganese salen imidos precludes establishing an equilibrium for protonation of the nitrido. Bounds for the pK_a values were determined by ^{1}H NMR in acetonitrile-d_3 at room temperature using acids of known pK_a values (see the Supporting Information). Notably, the pK_a values span ~9 units, with the basicity of the Mn(V) nitrido decreasing with an increasing charge of the bound cation.

The BDFEs for the imido N–H bonds are given in Table 1. Despite the changes in pK_a and reduction potential, the BDFE is relatively constant across the series, indicating that the positive shift in reduction potential is largely compensated by acidification of the imido. Although the determination of N–H bond strengths is challenging due to the reactive nature of the intermediate imido, these values are essential to predicting reactivity. A computational study by Cundari and co-workers on these complexes determined that an increase in charge at the bound cation resulted in an increase in the N–H BDFE and lower free energy barriers for hydrogen atom transfer (HAT) from methane.[72] Our experimentally determined BDFE values do not indicate an increasing N–H BDFE with higher cation charges. However, this may be due to our use of bracketed pK_a values due to the instability of the imidos. Still, we explored the hydrogen atom abstraction (HAA) reactivity of the Mn(VI) complexes with a hydrogen atom donor, 9,10-dihydroanthracene (DHA, BDFE(DMSO) = 72.9 kcal/mol)[18] (Scheme 1).

UV–visible spectroelectrochemistry was used to monitor the reactivity of complexes **A** and **1-Ba** with 100 equiv of DHA. Upon oxidation of **A** to the Mn(VI) species, only spectral changes that correspond to the formation of Mn(III) were observed (Figure S13). Recovery of the solution following electrolysis and analysis by ^{1}H NMR spectroscopy showed no evidence for the formation of anthracene, the expected product of hydrogen atom abstraction. For **1-Ba**, however, absorption bands corresponding to anthracene (340–380 nm)[73] increased in intensity during electrolysis (Figure S14), which was confirmed by ^{1}H NMR spectroscopy of the recovered solution. Spectroelectrochemical electrolyses of solutions of **1-La** with 100 equiv of DHA were unsuccessful due to the positive potential required to oxidize **1-La**, which resulted in the direct oxidation of DHA. Therefore, we performed chemical oxidation of **A**, **1-Ba,** and **1-La** with tris(2,4-dibromophenyl)-aminium hexachloroantimonate (Magic Green) under an inert atmosphere in *n*-PrCN at −40 °C. Following the *in situ* generation of the Mn(VI) nitrido and consumption of Magic Green, 10 equiv of DHA was added and the reaction mixture was stirred at −40 °C until no further reaction was observed. ^{1}H NMR spectroscopy was used to quantify the yield of anthracene (**2**) for each manganese complex (Scheme 1, inset table, and Figure S15). Two equivalents of manganese is required to form 1 equiv of anthracene (two HAT events); thus, the maximum possible yield of anthracene is 50%. The results of the chemical oxidation were variable due to competitive bimolecular coupling of the Mn(VI) complex, even at −40

°C (Figure S23). However, we note that chemical oxidation of **1-La** at −40 °C exhibited a minimal decay over 5 h.[30] The addition of cationic charge has a slightly positive effect on C–H activation. The hydrogen atom abstraction exhibited by **1-Ba** and **1-La** may be due to the inhibition of bimolecular coupling following oxidation to Mn(VI) due to the charge.[26] However, additional electrostatic interactions facilitating HAT cannot be ruled out.

Our results establish that BDFEs for the manganese imido N–H bonds change minimally with charge despite significant changes to $E_{1/2}$ and pK_a. We also demonstrate enhanced reactivity for HAT when a cation is bound using the hydrogen atom donor DHA. Our findings demonstrate the utility of electric fields for tuning the reduction potential, pK_a, and BDFE, while also differentially affecting hydrogen atom transfer. Future work will focus on understanding electrostatic effects for controlling different pathways for proton and electron transfer as well as C–H activation.

Supplementary Material

Refer to Web version on PubMed Central for supplementary material.

ACKNOWLEDGMENTS

We thank J. L. Lee in Prof. Borovik's group (UCI) for assistance in collecting EPR spectroscopy data. We also thank Dr. Felix Grun (UCI) for assistance with collecting mass spectrometry data.

Funding

T.C. was supported by NSF Award #15554744 and N.G.L. by NIH 3R01GM134047-02S1. N.G.L. also acknowledges support from the UC Presidential Postdoctoral Fellowship Program. J.Y.Y. also acknowledges support as a Sloan Foundation Fellow, a Canadian Institute for Advanced Research (CIFAR) Azrieli Global Scholar in the Bio-Inspired Solar Energy Program, and a Camille Dreyfus Teacher Scholar.

REFERENCES

(1). Smith JM Reactive Transition Metal Nitride Complexes. Prog. Inorg. Chem 2014, 58, 417–470.

(2). Sacramento JJD; Goldberg DP Factors Affecting Hydrogen Atom Transfer Reactivity of Metal–Oxo Porphyrinoid Complexes. Acc. Chem. Res 2018, 51 (11), 2641–2652. [PubMed: 30403479]

(3). Gunay A; Theopold KH C–H Bond Activations by Metal Oxo Compounds. Chem. Rev 2010, 110 (2), 1060–1081. [PubMed: 20143877]

(4). Larson VA; Battistella B; Ray K; Lehnert N; Nam W Iron and Manganese Oxo Complexes, Oxo Wall and Beyond. Nature Reviews Chemistry 2020, 4 (8), 404–419.

(5). Wiberg KB; Foster G The Stereochemistry of the Chromic Acid Oxidation of Tertiary Hydrogens1. J. Am. Chem. Soc 1961, 83 (2), 423–429.

(6). Breslow R; Balasubramanian KPK Alpha. of Triphenylcyclo-propene. Electrochemical Determination of an Inaccessible Equilibrium Constant. J. Am. Chem. Soc 1969, 91 (18), 5182–5183.

(7). Bordwell FG; Cheng JP; Harrelson JA Homolytic Bond Dissociation Energies in Solution from Equilibrium Acidity and Electrochemical Data. J. Am. Chem. Soc 1988, 110 (4), 1229–1231.

(8). Hammes-Schiffer S Proton-Coupled Electron Transfer: Moving Together and Charging Forward. J. Am. Chem. Soc 2015, 137 (28), 8860–8871. [PubMed: 26110700]

(9). Darcy JW; Koronkiewicz B; Parada GA; Mayer JM A Continuum of Proton-Coupled Electron Transfer Reactivity. Acc. Chem. Res 2018, 51 (10), 2391–2399. [PubMed: 30234963]

(10). Yosca TH; Rittle J; Krest CM; Onderko EL; Silakov A; Calixto JC; Behan RK; Green MT Iron(IV)Hydroxide PKa and the Role of Thiolate Ligation in C–H Bond Activation by Cytochrome P450. Science 2013, 342 (6160), 825–829. [PubMed: 24233717]

(11). Tyburski R; Hammarström L Strategies for Switching the Mechanism of Proton-Coupled Electron Transfer Reactions Illustrated by Mechanistic Zone Diagrams. Chem. Sci 2021, 13 (1), 290–301. [PubMed: 35059179]

(12). Tyburski R; Liu T; Glover SD; Hammarström L Proton-Coupled Electron Transfer Guidelines, Fair and Square. J. Am. Chem. Soc. 2021, 143, 560–576. [PubMed: 33405896]

(13). Goetz MK; Anderson JS Experimental Evidence for PKa-Driven Asynchronicity in C-H Activation by a Terminal Co(III)–Oxo Complex. J. Am. Chem. Soc 2019, 141 (9), 4051–4062. [PubMed: 30739450]

(14). Gao H; Groves JT Fast Hydrogen Atom Abstraction by a Hydroxo Iron(III) Porphyrazine. J. Am. Chem. Soc 2017, 139 (11), 3938–3941. [PubMed: 28245648]

(15). Barman SK; Yang M-Y; Parsell TH; Green MT; Borovik AS Semiempirical Method for Examining Asynchronicity in Metal–Oxido-Mediated C–H Bond Activation. Proc. Natl. Acad. Sci. U.S.A 2021, 118 (36), No. e2108648118. [PubMed: 34465626]

(16). Bell RP; Hinshelwood CN The Theory of Reactions Involving Proton Transfers. Proceedings of the Royal Society of London. Series A - Mathematical and Physical Sciences 1936, 154 (882), 414–429.

(17). Evans MG; Polanyi M Inertia and Driving Force of Chemical Reactions. Trans. Faraday Soc 1938, 34 (0), 11–24.

(18). Agarwal RG; Coste SC; Groff BD; Heuer AM; Noh H; Parada GA; Wise CF; Nichols EM; Warren JJ; Mayer JM Free Energies of Proton-Coupled Electron Transfer Reagents and Their Applications. Chem. Rev 2022, 122, 1–49. [PubMed: 34928136]

(19). Barman SK; Jones JR; Sun C; Hill EA; Ziller JW; Borovik AS Regulating the Basicity of Metal–Oxido Complexes with a Single Hydrogen Bond and Its Effect on C–H Bond Cleavage. J. Am. Chem. Soc 2019, 141 (28), 11142–11150. [PubMed: 31274298]

(20). Dhar D; Yee GM; Tolman WB Effects of Charged Ligand Substituents on the Properties of the Formally Copper(III)-Hydroxide ([CuOH]2+) Unit. Inorg. Chem 2018, 57 (16), 9794–9806. [PubMed: 30070473]

(21). Shaik S; Danovich D; Joy J; Wang Z; Stuyver T Electric-Field Mediated Chemistry: Uncovering and Exploiting the Potential of (Oriented) Electric Fields to Exert Chemical Catalysis and Reaction Control. J. Am. Chem. Soc 2020, 142 (29), 12551–12562. [PubMed: 32551571]

(22). Shaik S; Mandal D; Ramanan R Oriented Electric Fields as Future Smart Reagents in Chemistry. Nat. Chem 2016, 8 (12), 1091–1098. [PubMed: 27874869]

(23). Welborn VV; Pestana LR; Head-Gordon T Computational Optimization of Electric Fields for Better Catalysis Design. Nat. Catal 2018, 1 (9), 649–655.

(24). Léonard N; Dhaoui R; Chantarojsiri T; Yang JY Electric Fields in Catalysis: From Enzymes to Molecular Catalysts. ACS Catal 2021, 11, 10923–20932.

(25). Kang K; Fuller J; Reath AH; Ziller JW; Alexandrova AN; Yang JY Installation of Internal Electric Fields by Non-Redox Active Cations in Transition Metal Complexes. Chem. Sci 2019, 10 (43), 10135–10142. [PubMed: 32015820]

(26). Chantarojsiri T; Reath AH; Yang JY Cationic Charges Leading to an Inverse Free-Energy Relationship for N–N Bond Formation by MnVI Nitrides. Angew. Chem. Int. Ed 2018, 57 (43), 14037–14042.

(27). Eikey RA; Abu-Omar MM Nitrido and Imido Transition Metal Complexes of Groups 6–8. Coord. Chem. Rev 2003, 243 (1), 83–124.

(28). Berry JF Terminal Nitrido and Imido Complexes of the Late Transition Metals. Comments on Inorganic Chemistry 2009, 30 (1–2), 28–66.

(29). Mehn MP; Peters JC Mid- to High-Valent Imido and Nitrido Complexes of Iron. Journal of Inorganic Biochemistry 2006, 100 (4), 634–643. [PubMed: 16529818]

(30). Clarke RM; Storr T Tuning Electronic Structure To Control Manganese Nitride Activation. J. Am. Chem. Soc 2016, 138 (47), 15299–15302. [PubMed: 27933934]

(31). Man W-L; Lam WWY; Lau T-C Reactivity of Nitrido Complexes of Ruthenium(VI), Osmium(VI), and Manganese(V) Bearing Schiff Base and Simple Anionic Ligands. Acc. Chem. Res 2014, 47 (2), 427–439. [PubMed: 24047467]

(32). Xiang J; Jin X-X; Su Q-Q; Cheng S-C; Ko C-C; Man W-L; Xue M; Wu L; Che C-M; Lau T-C Photochemical Nitrogenation of Alkanes and Arenes by a Strongly Luminescent Osmium(Vl) Nitrido Complex. Communications Chemistry 2019, 2 (1), 1–11.

(33). Meyer K; Bendix J; Metzler-Nolte N; Weyhermüller T; Wieghardt K Nitridomanganese(V) and -(VI) Complexes Containing Macrocyclic Amine Ligands. J. Am. Chem. Soc 1998, 120 (29), 7260–7270.

(34). Keilwerth M; Grunwald L; Mao W; Heinemann FW; Sutter J; Bill E; Meyer K Ligand Tailoring Toward an Air-Stable Iron(V) Nitrido Complex. J. Am. Chem. Soc 2021, 143 (3), 1458–1465. [PubMed: 33430587]

(35). Du Bois J; Tomooka CS; Hong J; Carreira EM Nitridomanganese(V) Complexes: Design, Preparation, and Use as Nitrogen Atom-Transfer Reagents. Acc. Chem. Res 1997, 30 (9), 364–372.

(36). Chang CJ; Low DW; Gray HB Reversible Nitrogen Atom Transfer between Nitridomanganese(V) and Manganese(III) Schiff-Base Complexes. Inorg. Chem 1997, 36 (3), 270–271.

(37). Golubkov G; Gross Z Nitrogen Atom Transfer between Manganese Complexes of Salen, Porphyrin, and Corrole and Characterization of a (Nitrido)Manganese(VI) Corrole. J. Am. Chem. Soc 2005, 127 (10), 3258–3259. [PubMed: 15755125]

(38). Sengupta D; Sandoval-Pauker C; Schueller EC; Encerrado-Manriquez AM; Metta-Magana AJ; Lee W-Y; Seshadri R; Pintér B; Fortier S Isolation of a Bimetallic Cobalt(III) Nitride and Examination of Its Hydrogen Atom Abstraction Chemistry and Reactivity Towards H2. J. Am. Chem. Soc 2020, 142, 8233–8242. [PubMed: 32279486]

(39). MacLeod KC; McWilliams SF; Mercado BQ; Holland PL Stepwise N–H Bond Formation from N2-Derived Iron Nitride, Imide and Amide Intermediates to Ammonia. Chem. Sci 2016, 7 (9), 5736–5746. [PubMed: 28066537]

(40). Du Bois J; Hong J; Carreira EM; Day MW Nitrogen Transfer from a Nitridomanganese(V) Complex: Amination of Silyl Enol Ethers. J. Am. Chem. Soc 1996, 118 (4), 915–916.

(41). Ho C-M; Lau T-C; Kwong H-L; Wong W-T Activation of Manganese Nitrido Complexes by Bronsted and Lewis Acids. Crystal Structure and Asymmetric Alkene Aziridination of a Chiral Salen Manganese Nitrido Complex. J. Chem. Soc., Dalton Trans 1999, 15, 2411–2414.

(42). Yiu S-M; Lam WWY; Ho C-M; Lau T-C Facile N…N Coupling of Manganese(V) Imido Species. J. Am. Chem. Soc 2007, 129 (4), 803–809. [PubMed: 17243816]

(43). Liu Y; Lau T-C Activation of Metal Oxo and Nitrido Complexes by Lewis Acids. J. Am. Chem. Soc 2019, 141 (9), 3755–3766. [PubMed: 30707842]

(44). Wang D; Loose F; Chirik PJ; Knowles RR N–H Bond Formation in a Manganese(V) Nitride Yields Ammonia by Light-Driven Proton-Coupled Electron Transfer. J. Am. Chem. Soc 2019, 141 (12), 4795–4799. [PubMed: 30803234]

(45). Loose F; Wang D; Tian L; Scholes GD; Knowles RR; Chirik PJ Evaluation of Excited State Bond Weakening for Ammonia Synthesis from a Manganese Nitride: Stepwise Proton Coupled Electron Transfer Is Preferred over Hydrogen Atom Transfer. Chem. Commun 2019, 55 (39), 5595–5598.

(46). Kim S; Zhong H; Park Y; Loose F; Chirik PJ Catalytic Hydrogenation of a Manganese(V) Nitride to Ammonia. J. Am. Chem. Soc 2020, 142 (20), 9518–9524. [PubMed: 32339454]

(47). Pappas I; Chirik PJ Catalytic Proton Coupled Electron Transfer from Metal Hydrides to Titanocene Amides, Hydrazides and Imides: Determination of Thermodynamic Parameters Relevant to Nitrogen Fixation. J. Am. Chem. Soc 2016, 138 (40), 13379–13389. [PubMed: 27610465]

(48). Bezdek MJ; Pappas I; Chirik PJ Determining and Understanding N-H Bond Strengths in Synthetic Nitrogen Fixation Cycles. In Nitrogen Fixation; Nishibayashi Y, Ed.; Springer International: 2017; Topics in Organometallic Chemistry, pp 1–21. DOI: 10.1007/3418_2016_8.

(49). Rittle J; Peters JC N–H Bond Dissociation Enthalpies and Facile H Atom Transfers for Early Intermediates of Fe–N2 and Fe–CN Reductions. J. Am. Chem. Soc 2017, 139 (8), 3161–3170. [PubMed: 28140600]

(50). Chalkley MJ; Peters JC Relating N–H Bond Strengths to the Overpotential for Catalytic Nitrogen Fixation. Eur. J. Inorg. Chem 2020, 2020 (15–16), 1353–1357. [PubMed: 33071628]

(51). Johnson SI; Heins SP; Klug CM; Wiedner ES; Bullock RM; Raugei S Design and Reactivity of Pentapyridyl Metal Complexes for Ammonia Oxidation. Chem. Commun 2019, 55 (35), 5083–5086.

(52). Dunn PL; Cook BJ; Johnson SI; Appel AM; Bullock RM Oxidation of Ammonia with Molecular Complexes. J. Am. Chem. Soc 2020, 142 (42), 17845–17858. [PubMed: 32977718]

(53). Nieto I; Ding F; Bontchev RP; Wang H; Smith JM Thermodynamics of Hydrogen Atom Transfer to a High-Valent Iron Imido Complex. J. Am. Chem. Soc 2008, 130 (9), 2716–2717. [PubMed: 18266366]

(54). Reckziegel A; Pietzonka C; Kraus F; Werncke CG C–H Bond Activation by an Imido Cobalt(III) and the Resulting Amido Cobalt(II) Complex. Angew. Chem., Int. Ed 2020, 59 (22), 8527–8531.

(55). Xue X-S; Ji P; Zhou B; Cheng J-P The Essential Role of Bond Energetics in C–H Activation/Functionalization. Chem. Rev 2017, 117 (13), 8622–8648. [PubMed: 28281752]

(56). Iovan DA; Betley TA Characterization of Iron-Imido Species Relevant for N-Group Transfer Chemistry. J. Am. Chem. Soc 2016, 138 (6), 1983–1993. [PubMed: 26788747]

(57). Cowley RE; Holland PL C–H. Activation by a Terminal Imidoiron(III) Complex to Form a Cyclopentadienyliron(II) Product. Inorg. Chim. Acta 2011, 369 (1), 40–44.

(58). Ni C; Fettinger JC; Power PP Intramolecular C–H Activation by Putative Terminal Two-Coordinate Manganese(III) Imido Intermediates: Hydrogen Abstraction from a Phenyl Group. Organometallics 2010, 29 (1), 269–272.

(59). Shi H; Lee HK; Pan Y; Lau K-C; Yiu S-M; Lam WWY; Man W-L; Lau T-C Structure and Reactivity of a Manganese-(VI) Nitrido Complex Bearing a Tetraamido Macrocyclic Ligand. J. Am. Chem. Soc 2021, 143 (38), 15863–15872. [PubMed: 34498856]

(60). Shannon RD Revised Effective Ionic Radii and Systematic Studies of Interatomic Distances in Halides and Chalcogenides. Acta Cryst. A 1976, 32 (5), 751–767.

(61). Lane BC; McDonald JW; Basolo F; Pearson RG Reaction of Azidopentaammineiridium(III) Cation with Acid. Intermediate Formation of Coordinated Nitrene. J. Am. Chem. Soc 1972, 94 (11), 3786–3793.

(62). Gafney HD; Reed JL; Basolo F Photochemical Reaction of the Azidopentaammineiridium(III) Ion. Coordinated Nitrene Intermediate. J. Am. Chem. Soc 1973, 95 (24), 7998–8005.

(63). Lutz CM; Wilson SR; Shapley PA The First Imido Complex of Osmium(VI), [CpOs(NH)(CH2SiMe3)2][SO3CF3]. Organometallics 2005, 24 (13), 3350–3353.

(64). Scheibel MG; Abbenseth J; Kinauer M; Heinemann FW; Würtele C; de Bruin B; Schneider S Homolytic N–H Activation of Ammonia: Hydrogen Transfer of Parent Iridium Ammine, Amide, Imide, and Nitride Species. Inorg. Chem 2015, 54 (19), 9290–9302. [PubMed: 26192601]

(65). Kinauer M; Diefenbach M; Bamberger H; Demeshko S; Reijerse EJ; Volkmann C; Würtele C; Slageren J. van; Bruin B. de; Holthausen MC; Schneider S An Iridium(III/IV/V) Redox Series Featuring a Terminal Imido Complex with Triplet Ground State. Chem. Sci 2018, 9 (18), 4325–4332. [PubMed: 29780564]

(66). Chiu S-M; Wong T-W; Man W-L; Wong W-T; Peng S-M; Lau T-C Facile Nucleophilic Addition to Salophen Coordinated to Nitridoosmium(VI). J. Am. Chem. Soc 2001, 123 (50), 12720–12721. [PubMed: 11741454]

(67). Goken DM; Ischay MA; Peters DG; Tomaszewski JW; Karty JA; Reilly JP; Mubarak MS Alkyl Group Incorporation into Nickel Salen during Controlled-Potential Electrolyses in the Presence of Alkyl Halides. J. Electrochem. Soc 2006, 153 (3), No. E71.

(68). Cametti M; Dalla Cort A; Colapietro M; Portalone G; Russo L; Rissanen K Evidence of the Facile Hydride and Enolate Addition to the Imine Bond of an Aluminum–Salophen Complex. Inorg. Chem 2007, 46 (22), 9057–9059. [PubMed: 17892286]

(69). Meot-Ner M The Ionic Hydrogen Bond. 2. Intramolecular and Partial Bonds. Protonation of Polyethers, Crown Ethers, and Diketones. J. Am. Chem. Soc 1983, 105 (15), 4906–4911.

(70). Sharma RB; Blades AT; Kebarle P Protonation of Polyethers, Glymes, and Crown Ethers in the Gas Phase. J. Am. Chem. Soc 1984, 106 (3), 510–516.

(71). Chen Y; Rodgers MT Re-Evaluation of the Proton Affinity of 18-Crown-6 Using Competitive Threshold Collision-Induced Dissociation Techniques. Anal. Chem 2012, 84 (17), 7570–7577. [PubMed: 22881454]

(72). Najafian A; Cundari TR Effect of Appended S-Block Metal Ion Crown Ethers on Redox Properties and Catalytic Activity of Mn–Nitride Schiff Base Complexes: Methane Activation. Inorg. Chem 2019, 58 (18), 12254–12263. [PubMed: 31449394]

(73). Islangulov RR; Castellano FN Photochemical Upconversion: Anthracene Dimerization Sensitized to Visible Light by a RuII Chromophore. Angew. Chem., Int. Ed 2006, 45 (36), 5957–5959.

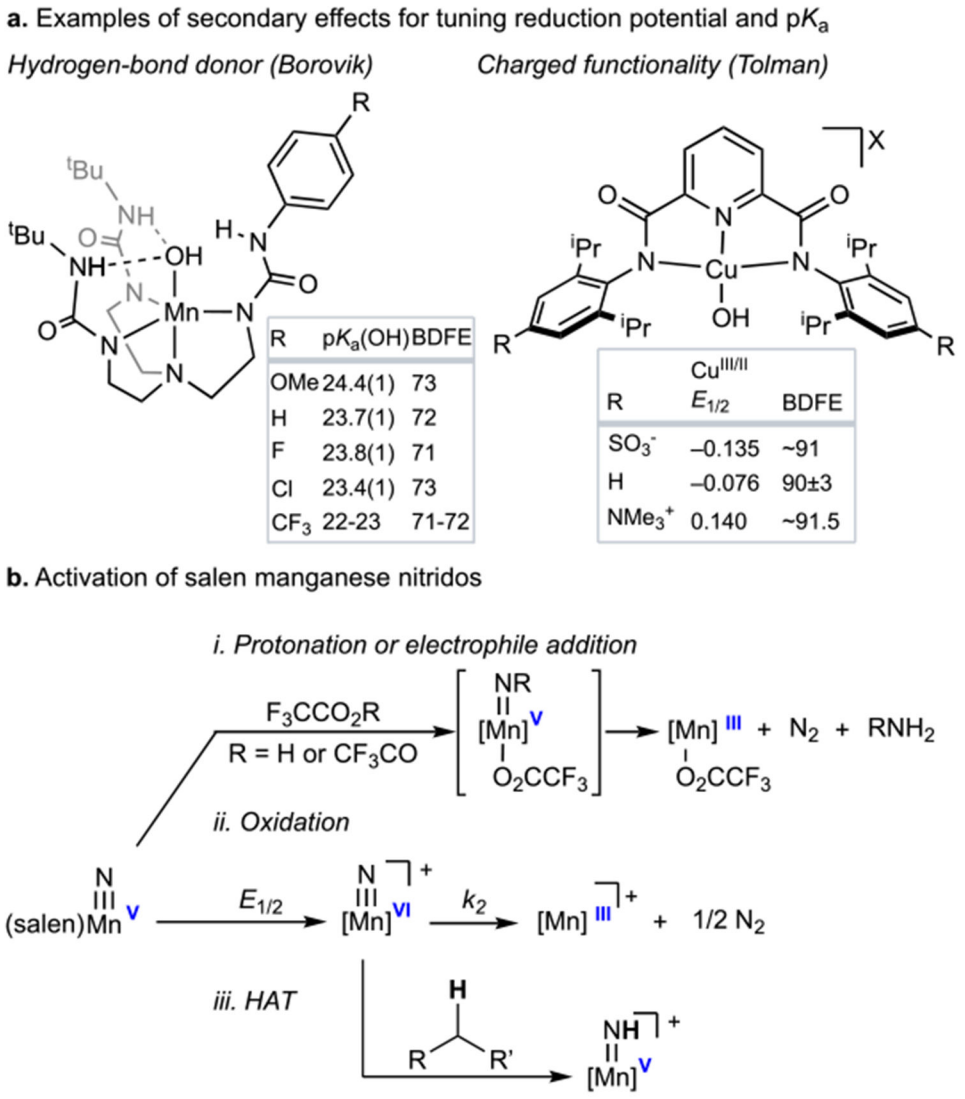

Figure 1.

(a) Secondary coordination sphere effects on $E_{1/2}$ or pK_a in metal hydroxides (refs 19 and 20). (b) Activation of salen manganese nitridos ((i) ref 42; (ii) refs 26 and 30; (iii) ref 72 and this work).

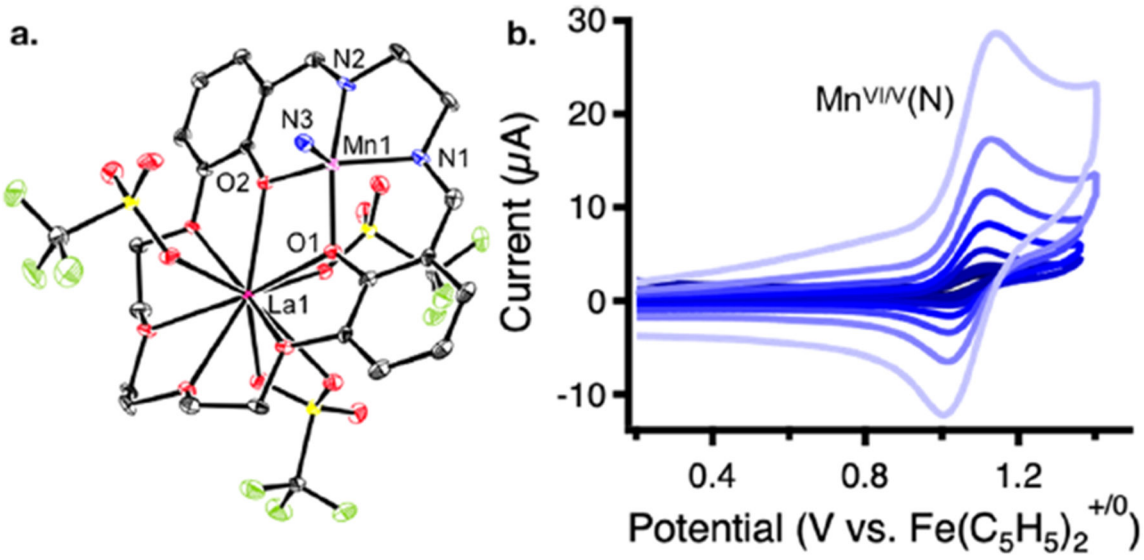

Figure 2.

(a) Solid-state molecular structure of **1-La** with 50% probability ellipsoids. Hydrogen atoms are omitted for clarity. See the Supporting Information for a full list of bond lengths and angles. (b) Scan-rate-dependent cyclic voltammetry of **1-La** (2 mM) showing $Mn^{VI/V}$ oxidation event (scan rates 10–2500 mV/s, 0.2 M $TBAPF_6$, CH_3CN).

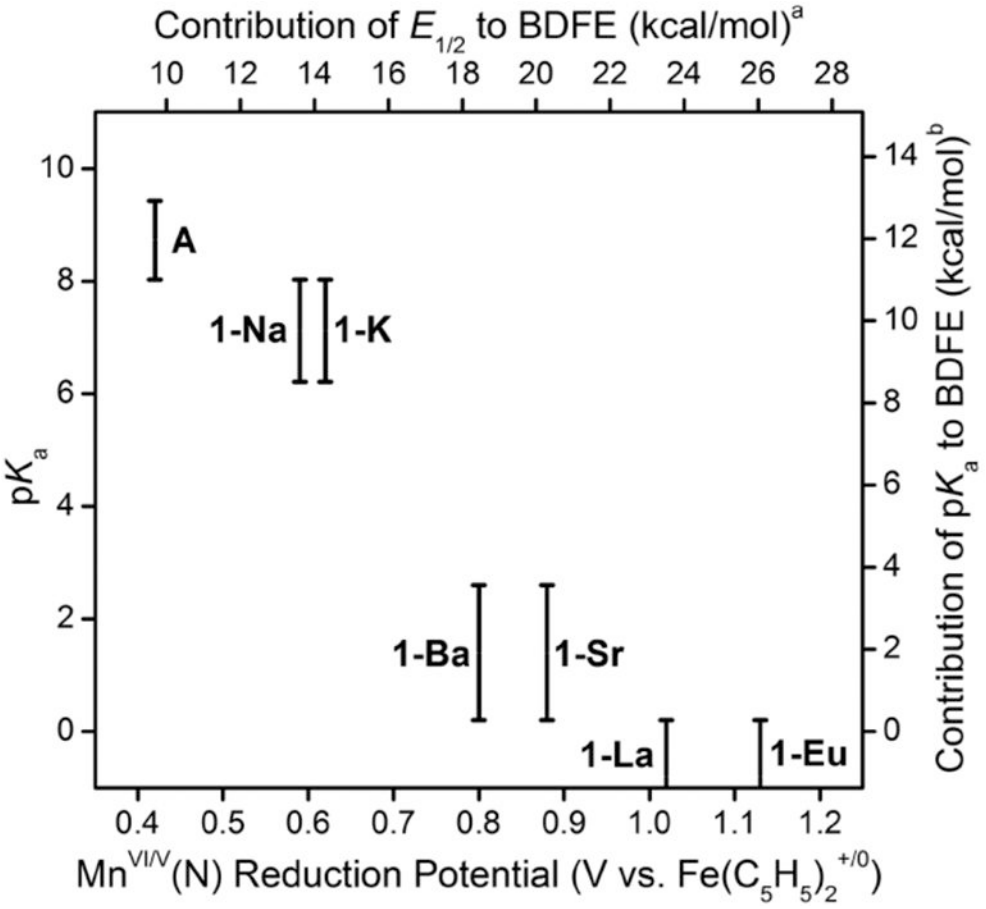

Figure 3.

Plot showing the compensatory relationship between the $Mn^{VI/V}$ $E_{1/2}$ and pK_a for complexes with a cationic charge and contribution to BDFE. Axis values were calculated as (a) 23.06($E_{1/2}$) and 0) 1.37(pK_a) as shown in eq 1 in Chart 1.

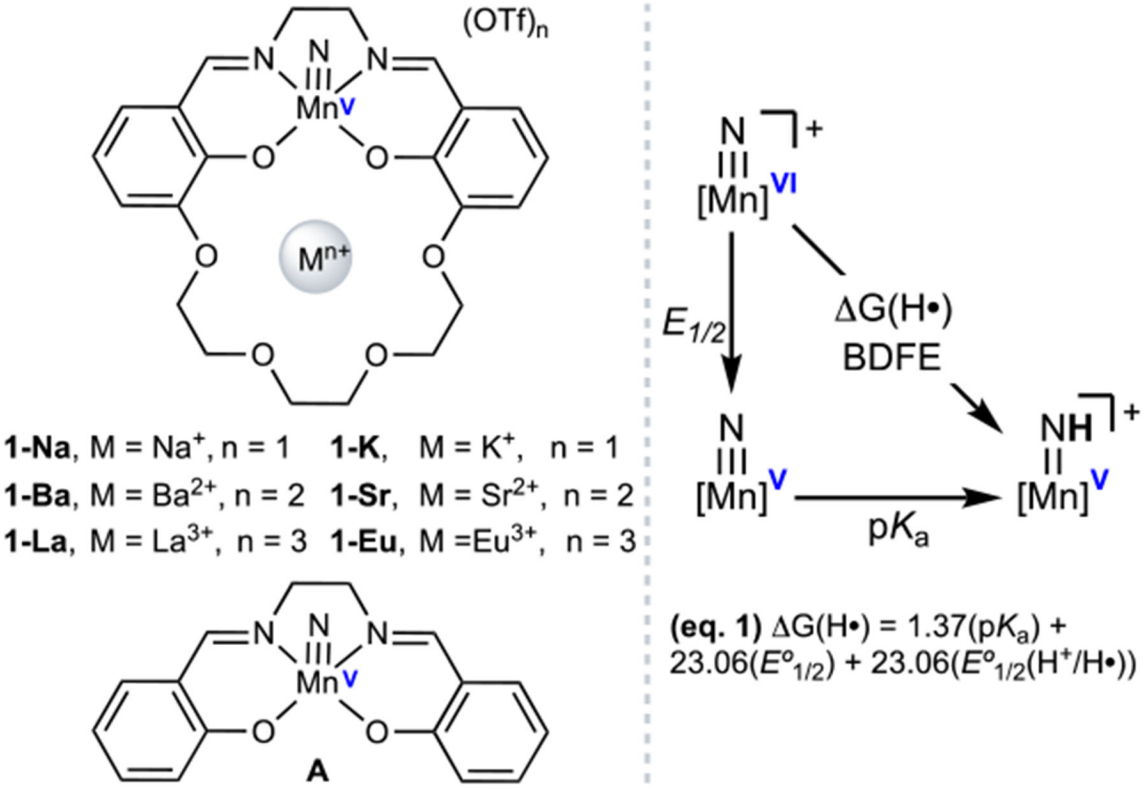

Chart 1.

(Left) Manganese Nitrido Complexes and (Right) Thermodynamic Properties Investigated in This Study

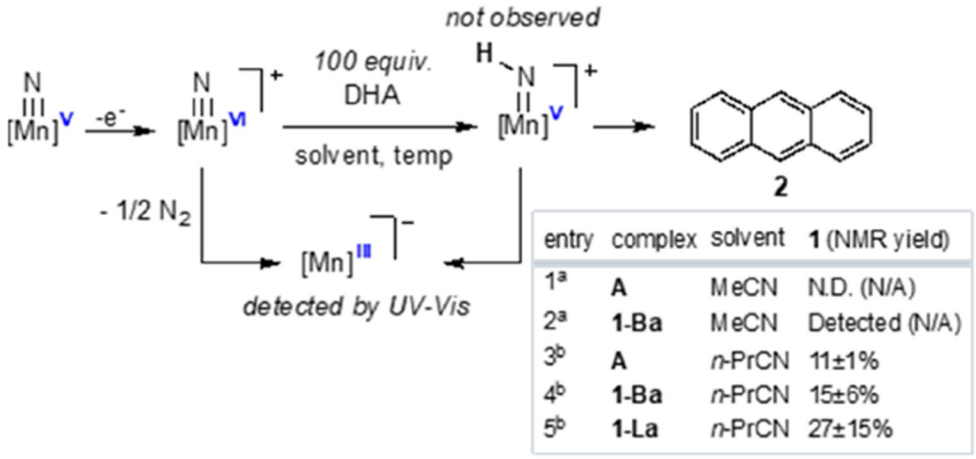

entry	complex	solvent	**1** (NMR yield)
1[a]	**A**	MeCN	N.D. (N/A)
2[a]	**1-Ba**	MeCN	Detected (N/A)
3[b]	**A**	*n*-PrCN	11±1%
4[b]	**1-Ba**	*n*-PrCN	15±6%
5[b]	**1-La**	*n*-PrCN	27±15%

Scheme 1. Reaction of Manganese Complexes with DHA following Oxidation

[a]Reaction performed by spectroelectrochemical UV–vis in MeCN at 20 °C. [b]Reaction performed by chemical oxidation with 1 equiv of tris(2,4-dibromophenyl)aminium hexachloroantimonate in *n*-PrCN at −40 °C. See the Supporting Information for experimental details.

Table 1.

Summary of Thermodynamic Parameters

complex	$E_{1/2}$ [c]	pK_a [d]	N–H BDFE [e]
A [a]	0.43	8.0–9.4	73–75
1-Na [a]	0.59	6.2–8.0	75–77
1-K [a]	0.62	6.2–8.0	75–78
1-Ba [a]	0.80	0.2–2.6	71–75
1-Sr [a]	0.88	0.2–2.6	73–76
1-La [b]	1.02	<0.2	<76
1-Eu [b]	1.13	<0.2	<79

[a] Reference 26.

[b] This work.

[c] In V; $Mn^{VI/V}$(N) couple vs $Fe(C_5H_5)_2^{+/0}$ in MeCN.

[d] Protonation of nitrido complexes in MeCN-d_3 at 20 °C as determined by ^{1}H NMR.

[e] In kcal/mol using experimentally measured $E_{1/2}$ and pK_a (eq 1 in Chart 1).